

NASA Technical Memorandum 87747

NASA-TM-87747 19860020160

**INTERACTION OF AIRBORNE AND STRUCTUREBORNE
NOISE RADIATED BY PLATES
VOLUME II -- EXPERIMENTAL STUDY**

MICHAEL C. McGARY

JULY 1986



National Aeronautics and
Space Administration

Langley Research Center
Hampton, Virginia 23665

LIBRARY COPY

AUG 4 1986

**LANGLEY RESEARCH CENTER
LIBRARY, NASA
HAMPTON, VIRGINIA**



NF01631

SUMMARY

An experimental study was undertaken in order to further the understanding of the interaction of airborne and structureborne noise radiated by aircraft materials. The results of the study corroborate the findings of an earlier analytical study by showing that the noise radiation of vibrating plates due to combined airborne and structureborne inputs possesses a strong synergistic nature. The large influence of the interaction between the airborne and structureborne inputs has been hitherto ignored by researchers of aircraft interior noise problems.

1. INTRODUCTION

In the past, reseachers investigating the area of aircraft interior noise in propeller driven aircraft have tended to restrict their efforts to one of two aspects of the problem, viz. (1) the study of the transmission of airborne noise and its control or (2) the study of structureborne noise transmission and its control. This approach has neglected the possible phase dependent interaction of the fully coherent airborne and structureborne components. In part I of this paper [1] the theoretical basis and the computational results of an analytical study were presented which examine the interaction between the airborne and structureborne noise radiated by plates. It is shown in references [1] and [2] that the phase dependent interaction between the airborne and structureborne inputs can be represented mathematically as cross terms in both the dynamic and acoustic analyses. The results of the analytical study [1,2] suggest that the noise radiation of vibrating plates in the low frequency regime due to combined airborne and structureborne inputs possesses a stong synergistic nature. An experimental study was performed in order to verify the behavior predicted by the analytical model of reference [1]. This paper first presents the details of the measurement theory and apparatus that were used in the experimental

study and then presents selected results that were obtained from the experiments.

2. PROBLEM APPROACH

Simple isotropic rectangular plates served as the test vehicle for the studies. The plates chosen for study were constructed of 0.8 mm (0.032 in) thick AA 2024 aluminum (surface density of 2.22 kg/m^2). The physical dimensions of the plates were chosen to be 0.406 m x 0.241 m (16 in x 9.5 in). Plates were chosen for study because they possess most of the vibrational and sound radiative properties that are exhibited by aircraft sidewalls.

The plates were mounted in a rigid baffle constructed of particle board and then placed in a transmission loss (TL) apparatus. The approach was to subject the plates to fully coherent acoustic and vibrational inputs on the source room side of the TL apparatus and then measure the resulting sound power on the receiving side of the TL apparatus.

The effects of several parameters on the interaction between the airborne and structureborne components were investigated. Parameters studied included the relative magnitude and phase of the acoustic and vibrational inputs, the location of the structureborne input, and the level of structural damping.

3. THEORY OF MEASUREMENT

The sound power radiated by a plate due to combined airborne and structureborne inputs has been shown, in theory [1,2], to be a function of several parameters including the relative magnitude and phase of the inputs, the path of the inputs, and the level of structural damping. The present section deals with how the sound power radiated by a plate can be measured in theory.

The time averaged sound power radiated by the surface of a structure is given by the equation

$$\langle \Pi \rangle_t = \iint \langle \vec{I} \cdot \vec{n} \rangle_t dS = \langle \vec{I} \cdot \vec{n} \rangle_{r,t} S, \quad (1)$$

where

\vec{I} = the acoustic intensity vector measured at the surface,

\vec{n} = the unit normal vector to the surface, and

S = the surface area of the structure.

In this experimental study the acoustic intensity vector normal to the surface was measured using a two microphone, cross spectral, acoustic intensity probe. The theoretical basis for this type of probe is summarized in reference [3]. The acoustic intensity is calculated from the imaginary part of the one-sided cross spectral density between the two signals produced by two closely spaced

microphones. The equation for the time averaged acoustic intensity is given by

$$\langle I \rangle_t = Q_{12} \Delta f / (\rho_o \omega \Delta x) , \quad (2)$$

where

Q_{12} = quadrature spectral density between the two microphone signals,

Δf = the frequency resolution (bandwidth) in Hertz,

ρ_o = the density of the acoustic fluid medium,

ω = the radian frequency of the acoustic disturbance,

Δx = the spacing between the two microphones.

The quadrature spectral density, Q_{12} , can be easily measured with a dual channel or a multichannel Fast Fourier Transform (FFT) analyzer. The remaining terms in equation (2) are either constant or are parameters (such as bandwidth) which are set by the FFT analyzer. The space-time averaged acoustic intensity is found in practice by slowly sweeping the two microphone acoustic intensity probe near the surface of the intended measurement area as the FFT analyzer calculates the time averaged cross spectral density between the microphone signals. Thus, the space averaging and the time averaging of the cross spectral density is performed simultaneously. (The results of a study which compares this method of space-time average with fixed point measurements for obtaining the space-time averaged acoustic

intensity is presented in reference [4].) Once the space-time averaged cross spectral density between microphone signals is measured, the space-time averaged acoustic intensity may be calculated as a function of frequency using equation (2) by computer, or by the FFT analyzer (depending on the analyzer's level of sophistication). The total sound power radiated is then calculated by multiplying the space-time averaged intensity by the measurement area. (See equation (1).) The measurement area may be the surface area of the structure, providing that the intensity probe is swept close enough to the surface, and if there are no stiffeners, etc.. attached to the intended measurement surface.

4. EXPERIMENTAL APPARATUS

The experimental study was performed using the NASA Langley Research Center's acoustic transmission loss apparatus. This facility is a hard walled, two room facility designed for acoustic transmission loss measurements using the classical room acoustics method. The two rooms have an adjoining wall which is designed so that simple or built-up aircraft panels can be mounted between the two rooms. With this arrangement, test panels could be subjected to the desired acoustic and vibrational inputs in the source room while the sound power radiated by the panels could be measured in the receiving room. Since the analytical model

discussed in reference [1] assumes that the test panels radiate sound to an acoustic free field condition, and since the accuracy of intensity measurements are in question under reverberent conditions, the receiving room of the transmission loss apparatus was modified to semi-anechoic conditions. This was accomplished by covering the back wall of the receiving room with 0.91 m deep acoustic wedges and covering the floor of the room with 0.46 m deep polyurethane foam acoustic wedges. No further modifications of the transmission loss apparatus were required to perform the measurements. (Additional information regarding the acoustic properties of the NASA acoustic transmission loss apparatus is available in references [5] and [6].)

A special apparatus for mounting the test panels was constructed so that the experimental conditions would emulate the conditions assumed for the analytical modeling. The apparatus consisted of a speaker box which completely enclosed the incident side of the test panels. Two small holes were drilled through the enclosure so that a steel rod and shaker could be attached to the test panels in one of two locations. The test panels were then clamped in the mounting brackets seen in figure (1) in front of six 10 cm (4 in) diameter loudspeakers. The mounting brackets, shown in close-up in figure (2), were constructed with a rubber O-ring type material so that the test panels would have some

rotational degree of freedom, thus approximating the simply supported conditions assumed in the analytical modeling.

The array of six loudspeakers shown in figure 1 were used to produce a normally incident, spatially uniform acoustic (airborne) input to the test panels. The loudspeakers were positioned 5.7 cm from the surface of the test panels, thus insuring that the acoustic resonances in the cavity between the panels and the speakers have natural frequencies much greater than 1000 Hz. The elimination of any significant influence due to the cavity modes helped to produce an acoustic input that was nearly uniform over the 0-1000 Hz frequency range. The small distance between the speakers and the panels also insured that the direct sound field from the speakers would overwhelm the effects of any cross modes in the cavity, thereby approximating the spatially uniform conditions. A preliminary set of measurements was performed on the loudspeakers to insure that they were in phase and produced the same level of sound over the 0-1000 Hz range. The range of the measured space time averaged acoustic intensity radiated by the six loudspeakers to the free field over the 0-1000 Hz frequency range is given in figure (3).

A 44.5 N (force) vibration shaker was used in conjunction with a 6.4 mm diameter steel rod to simulate the point vibrational (structureborne) input. The shaker was mounted

outside of the speaker box by suspending it freely with bungee cord that was attached to a scaffold apparatus. This arrangement ensured that the shaker-rod-panel system had a low natural frequency and reduced any d.c. component of the point forcing function to a minimum. The threaded rod was attached to the panel, in each case, by drilling a hole in the panel, slipping the rod through the hole, and tightening a hex nut down on each side of the panel. A typical example of the forcing function produced by this apparatus over the 0-1000 Hz frequency range is given in figure (4).

5. INSTRUMENTATION AND DATA ACQUISITION

A block diagram of the instrumentation used for the measurements is shown in figure (5). The specifications for the instruments are given in reference [2].

The white noise generator, shown in the figure, provided a broadband random signal (0-5000 Hz) that was used to simultaneously drive both the loudspeakers and the shaker system. This single source ensured that the airborne and structureborne inputs were fully coherent. The signal was filtered using both a high pass and a low pass filter so that the sound radiated by the panels would be concentrated in the 100-1000 Hz frequency range. A signal attenuator was used to adjust the level of the airborne input so that the relative amounts of airborne and structureborne noise radiated by the panels were roughly equal.

A two microphone acoustic intensity probe was used to measure the sound power radiated by the panels. The probe consisted of two 1.27 cm diameter high gain microphones in a face-to-face configuration. A solid nylon cylindrical spacer between the microphones provided a constant separation distance of 50 mm. This separation distance between microphones ensures that the sound power measurements are accurate over the 100-1000 Hz frequency range. Below 100 Hz the sound power measurements are suspect due to phase mismatch errors. Above 1000 Hz the sound power measurements are inaccurate due to finite difference error. (See reference [3] for details.) Since the microphone interchange technique was used for the measurements, the intensity probe was used twice for any given measurement of space-time averaged acoustic intensity. (This method reduces the phase mismatch error [3].) The FFT analyzer obtained 200 ensemble averages for each of the two passes of the intensity probe. Thus, a total of 400 ensemble averages were used to obtain the time averaged intensity. The space average was obtained by slowly sweeping the intensity probe near the surface of the panel.

Calibration of the microphones were performed using a sound level calibrator. The transducers were calibrated prior to the measurement on each day that a measurement was to take place. The voltages produced by the transducers due

to a known input were read on the digital voltmeter shown in figure (5). Calibration was then implemented by adjusting the gain on the microphone amplifiers so that the gain factors were always 0.1 volts/Pascal for the microphones. The oscilloscope shown in figure (5) was used to insure that the signals received during calibration were free of distortion, thus making certain that the transducers were in acceptable operating condition. The scanner shown in figure (5) was utilized during both calibration and measurement so that any of the data channels could be monitored without disconnecting or reconnecting any wire leads.

The data acquisition was performed by the 8-channel FFT analyzer. Two of the analyzer's 8 channels were used for the microphones and two channels were used to monitor the white noise input signal and the signal provided by the force gauge. In addition to the data obtained by the analyzer, the atmospheric conditions including temperature and barometric pressure were recorded each day and entered into the data files. The atmospheric data were used later in the computations to calculate the density, ρ_0 , of the fluid medium. (This quantity is used in calculating the sound power radiated by the plate.)

6. RESULTS

This section contains selected results of the experimental studies. The experimental results presented are

intended to verify the trends predicted in reference [1]. Since the electronic equipment necessary for controlling the relative magnitude and phase of the inputs as a function of frequency was unavailable, the corresponding analytical cases presented in reference [1] and experimental cases presented here are not exactly the same. Although the analytical and experimental results can not be compared quantitatively, the results can be compared in a qualitative sense by showing that predicted and observed trends are similar.

The experimental results presented in this section were obtained using the apparatus discussed earlier. The results that demonstrate the effects produced by changes in the relative phase of the inputs were obtained by reversing the polarity of the shaker system. This was accomplished simply by switching the wire leads connecting the shaker to the input signal. This reversal of the polarity of the shaker is tantamount to changing the relative phase between the acoustic and vibrational inputs by 180 degrees from the existing phase difference at all frequencies.

Several conditions were consistently maintained for all of the experimental results shown. The same input signal was applied to both the array of speakers and the shaker so that the two inputs were fully coherent. The input signal was filtered so that the input was approximately uniform

over the 100-1000 Hz frequency range. The overall gain factors of the acoustic and vibrational inputs were adjusted so that the airborne sound power component would be dominant in some frequency ranges while the structureborne sound power component was dominant in other ranges. Also, in order to match the resolution of the analytical results, the FFT analyzer was set with a constant bandwidth of 2 Hz. Finally, unless explicitly stated otherwise, the experimental results presented here were measured data on an aluminum plate for the case of an approximately uniform normal acoustic load and a point vibrational load located at the coordinates of $\alpha_1 = 0.060$ m and $\alpha_2 = 0.135$ m.

The results that follow are divided into three sections. In the first section, the effects of the relative magnitudes and phase of the inputs are investigated. In the second section, the effects produced by changing the shaker location (altering the path of the structureborne input) are examined. Finally, the third section examines the effects of adding damping treatment to the aluminum plate.

6.1 EFFECTS OF RELATIVE MAGNITUDE AND PHASE

Figure (6) shows the measured sound power levels produced by the aluminum plate due to the acoustic and vibrational inputs acting independently. This figure shows that, in this case, the structureborne component of the sound power is dominant in several small discrete frequency

regions while the airborne component is dominant over most of the frequency range.

The sound powers produced by combining the airborne and structureborne components are shown in figures (7) and (8). The two curves in figure (7) show the results of first summing the individual airborne and structureborne components, and then combining the airborne and structureborne inputs with positive polarity on the shaker. The two curves in figure (8) show the results of first summing the individual airborne and structureborne components, and then combining the inputs with negative polarity on the shaker. These figures show that the sum of the results of the individual inputs is roughly equivalent to the results obtained by combining the inputs. The largest differences between the combined sound power curves and the sum of the individual sound power components are seen to occur in frequency regions where the sound power is dominated by the structureborne component. Moderate differences are seen to occur in frequency regions where the curves reach a local minimum. These differences are most certainly a reflection of the influence of the interaction between the airborne and structureborne inputs in those localized frequency ranges.

6.2 EFFECTS OF ALTERING THE INPUT PATHS (SHAKER LOCATION)

Figures (9) through (11) show the measured data that were obtained from the aluminum plate for the case of an

approximately uniform acoustic load and a point vibrational load located at the new coordinates of $\alpha_1 = 0.121$ m and $\alpha_2 = 0.203$ m. These coordinates place the vibrational point load at the center of the plate, thus driving exactly the same modes as the acoustic input.

Figure (9) shows the sound power levels produced by the plate due to independent acoustic and vibrational loads. This figure shows that the structureborne component of the sound power is dominant in several small discrete frequency regions while the airborne component is dominant over most of the frequency range. A smoother structureborne curve is expected in this case, since the shaker drives only the odd modes of the panel. Note that the structureborne sound power curve is in fact smoother than the curves obtained when the panel was driven near the corner.

The measured sound powers of the aluminum plate produced by combining these two inputs are shown in figures (10) and (11). These figures again show that the sum of the results of the individual inputs is roughly equivalent to the results obtained by combining the inputs. Very large differences in the curves (as much as 5 dB) are seen to occur, however, in some frequency regions. These differences can again be explained by the phase dependent interaction between the airborne and structureborne inputs. Note that figures (10) and (11) show larger differences between

the sound power curves than was observed in figures (7) and (8). This suggests that the interaction between the airborne and structureborne components becomes more important if the two inputs drive the same modes of the structure. Comparison of figures (10) and (11) show that the airborne-structureborne interaction can account for as much as a 10 dB overall variation in the sound power level in some frequency ranges.

6.3 EFFECTS OF ADDED DAMPING

Figures (12) through (14) show the measured results that were obtained from the aluminum plate with damping tape added to the plate. The self-adhesive damping tape consisted of single layer of polystyrene type foam material with an outer layer of aluminum foil. The tape added approximately 1.44 kg/m^2 to the surface density of the panel. This type of damping tape is commercially available from several manufacturers and is routinely used to dampen vibration of the sidewalls of general aviation aircraft.

Figure (12) shows the sound power levels produced by the damped plate due to independent acoustic and vibrational loads. This figure shows that the airborne source is dominant over nearly the entire frequency range.

The sound powers produced by combining these two inputs are shown in figures (13) and (14). These figures show that the combined sound power is largely influenced by the phase

dependent interaction between the airborne and structureborne inputs. The two figures again show that in some frequency regions the phase dependent terms can cause the sound power radiated by the plate to vary over a 10 dB range.

As predicted by the analytical study [1], the added damping causes the sound power curves to appear much smoother over the frequency range when compared to the undamped case. The increased smoothness of the curves can be explained in terms of the forced response of the individual modes of the plate. Heavily damped modes have a smaller quality factor than undamped modes and therefore, the influence of each of the damped modes extends over a much larger frequency region. This feature of the damped modes acts like a moving band average and is responsible for the smoothing effect observed figures (12) through (14). This increased smoothness makes the effects of the airborne-structureborne interaction particularly evident. Furthermore, from figures (13) and (14), one can conclude that the addition of damping to the structure does not diminish the relative importance the airborne-structureborne interaction. In fact, the results suggest that, at least in terms of overall sound power levels, the added damping tends to magnify the airborne-structureborne interactive effects.

7. CONCLUDING REMARKS

The results of the experimental study indicate that the phase dependent interaction between the airborne and structureborne inputs can have a very significant effect on overall noise radiation. The results show that in some frequency ranges the interactive terms can be as large or larger than the independent airborne and structureborne terms. The results also suggest that the interactive terms become more important when the airborne and structureborne inputs drive the same modes and/or when the individual modes of the structure influence a large frequency region (as in the case of the damped plate). Each of these results corroborates similar findings obtained in the analytical study [1].

The results of this experimental study, along with the analytical results [1], suggest that the interaction of airborne and structureborne noise may be responsible for a significant amount of the overall noise generation and/or noise suppression in the cabins of propeller driven aircraft. It might be argued that because of the multiplicity of sound sources in an aircraft cabin, the space average of these interactive effects tends to zero. It is quite possible, however, that the interactive effects play an important role at discrete points in the aircraft cabin. Since the ear perceives sound at (roughly) discrete points, it may be that the interactive effects are significant.

Earlier studies by other reseachers [7,8] have shown that the addition of the structureborne inputs to the airborne component can double the measured sound pressure levels in some aircraft. These earlier studies, however, failed to show the exact mechanism by which the increase in the noise levels (due to combining the inputs) occurs. At the present time, it is not known whether these observed increases in the noise levels are due to independent structureborne components or if they are simply a reinforcement of the airborne component through airborne-structureborne interaction. At first glance, it seems unlikely that the interactive effects could consistently increase the noise levels throughout the space of an aircraft cabin. Recent experimental results published by Fuller [9], however, suggest that the interactive effects between an acoustic input and a point vibrational input can in fact decrease the noise levels inside a cylinder in a spatially uniform fashion. Fuller's results lend more credence to the suggestion that important airborne-structureborne interactions may occur in propeller driven aircraft.

In the past 7 or 8 years [10], a considerable number of analytical studies and complicated computer models have been based on the premise that the interior noise problems in propeller driven aircraft are solely airborne in origin. If it turns out that the airborne-structureborne interactive

effects are an important factor in the interior noise of propeller driven aircraft, then many of the observed discrepancies between theory and experiment in recent studies might be explained in terms of these interactive effects. If this proves to be the case, researchers should begin to rethink their approach to aircraft interior noise problems. Additionally, if it can be shown that the airborne-structureborne interaction in aircraft structures is large, it may be possible to reduce interior noise that is primarily airborne in origin by using vibrational inputs to cancel much of the sound. Thus, active vibration control may be a viable option for controlling and reducing interior noise in propeller driven aircraft.

REFERENCES

1. M.C. McGary 1985 Submitted for publication in the Journal of Sound and Vibration, Interaction of Airborne and Structureborne Noise Radiated by Plates Part I - Analytical Study.
2. M.C. McGary 1985 Ph.D. Dissertation, Stanford University, Separation of Airborne and Structureborne Noise Radiated by Plates Constructed of Conventional and Composite Materials with Applications for Prediction of Interior Noise Paths in Propeller Driven Aircraft.
3. J.Y. Chung 1981 Recent Developments in Acoustic Intensity Measurement, Cent. Tech. Ind. Mech., pp. 1-10, Fundamental Aspects of the Cross Spectral Method of Measuring Acoustic Intensity.
4. M. Bockhoff 1984 Proceedings of INTER-NOISE 84, pp. 1173-1176, Some Remarks on the Continuous Sweeping Method in Sound Power Determination.
5. M.C. McGary 1982 NASA Technical Memorandum 83275, Sound Field Diffusivity in NASA Langley Research Center Hardwalled Acoustic Facilities.
6. F.W. Grosveld 1983 NASA Contractor Report 172153, Characteristics of the Transmission Loss Apparatus at NASA Langley Research Center.
7. V.L. Metcalf and W.H. Mayes 1983 S.A.E. Technical Paper 830735, Structureborne Contribution to Interior Noise of Propeller Aircraft.
8. J.F. Unruh and D.C. Scheidt 1979 S.A.E. Technical Paper Series 790626, Engine Induced Structure-Borne Noise in a General Aviation Aircraft.
9. C.R. Fuller 1985 110th Meeting of the Acoustical Society of America, Experiments on Reduction of Aircraft Interior Noise using Active Control of Fuselage Vibration.
10. J.S. Mixson and C.A. Powell 1984 AIAA/NASA 9th Aeroacoustics Conference, Review of Recent Research on Interior Noise of Propeller Aircraft.

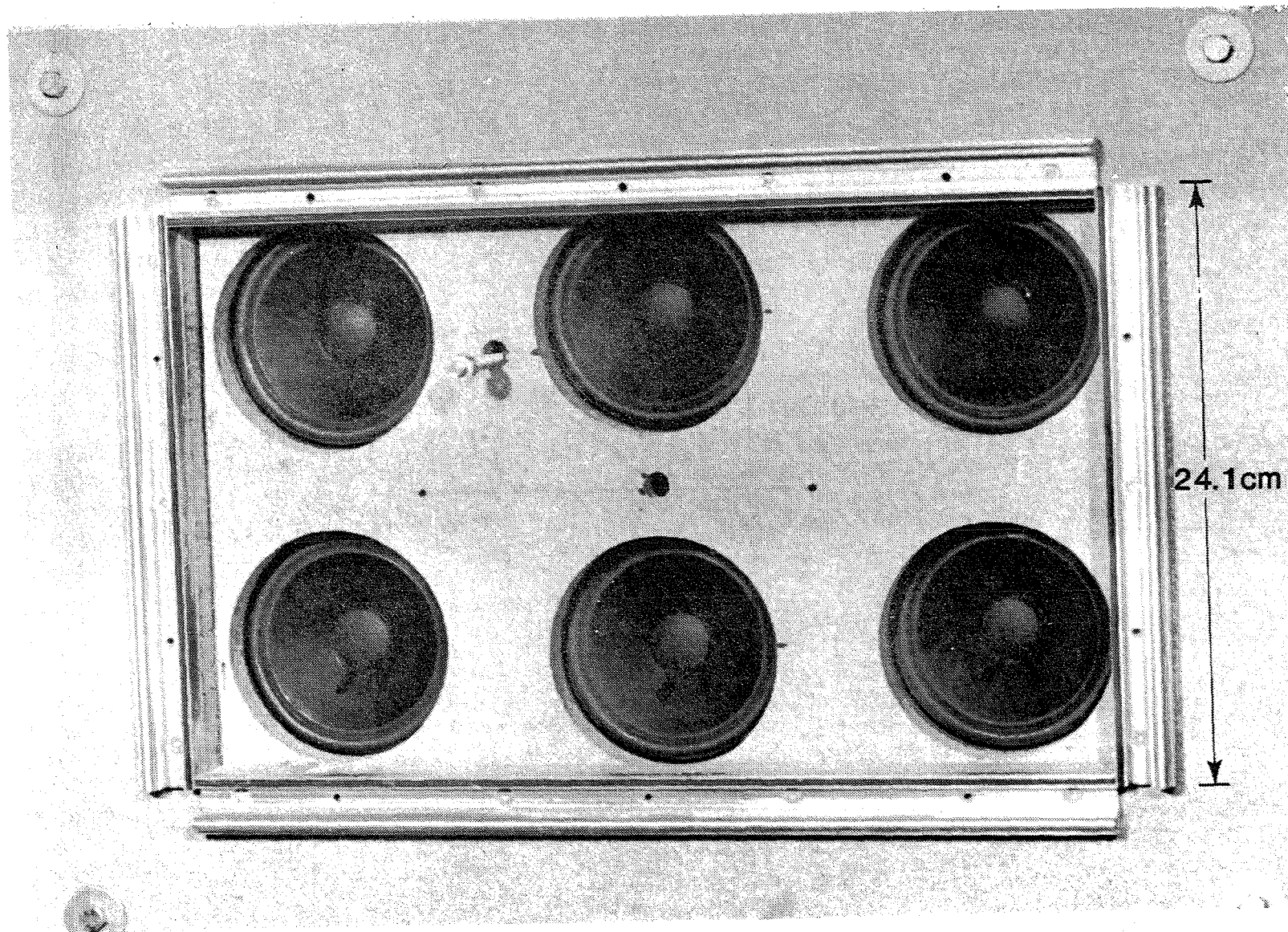


Figure 1 -- Mounting brackets for the panels and array of six loudspeakers.

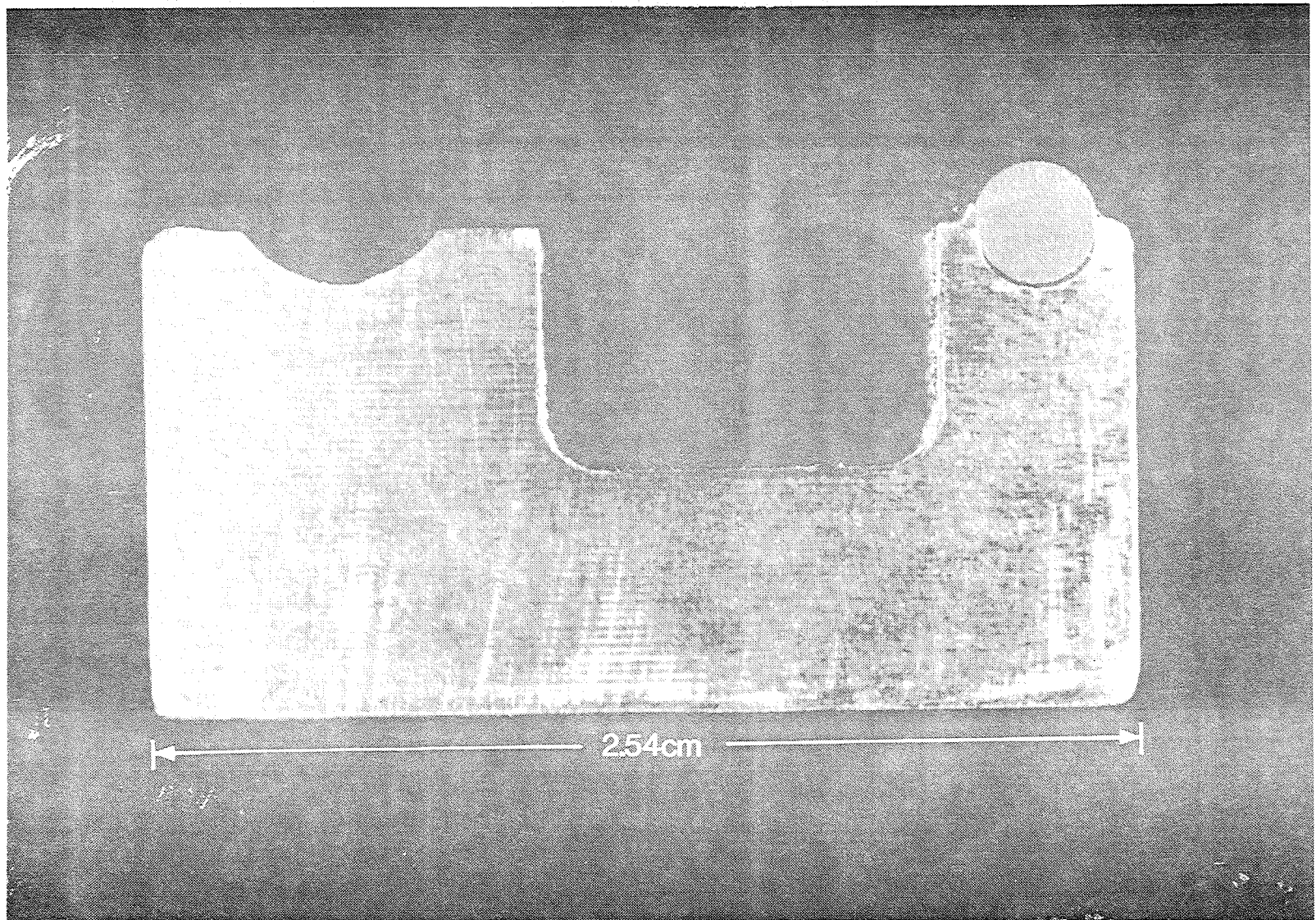


Figure 2 -- Close-up cross sectional view of the mounting brackets for the panels.

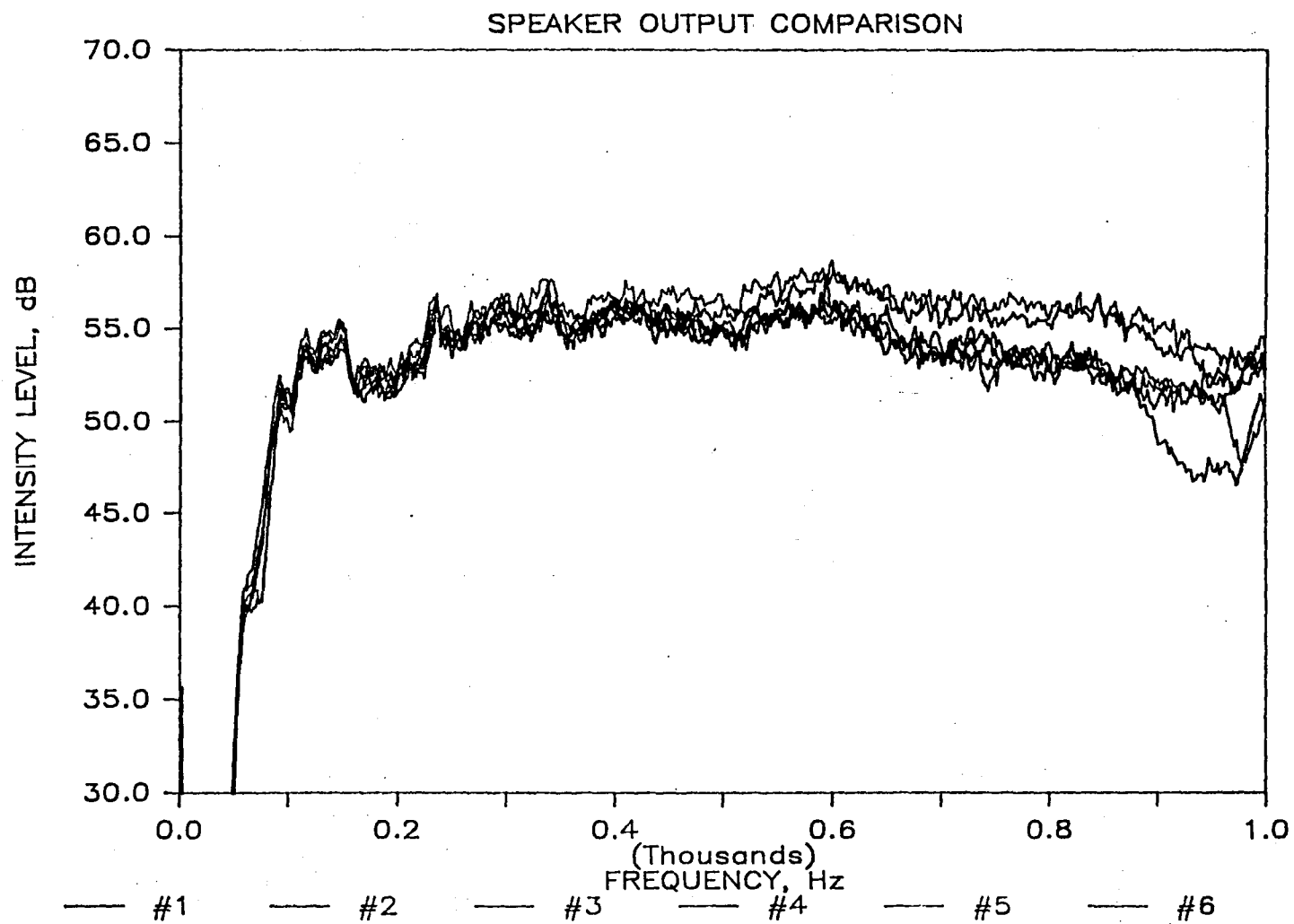


Figure 3 -- Acoustic intensity radiated by each of the six loudspeakers.

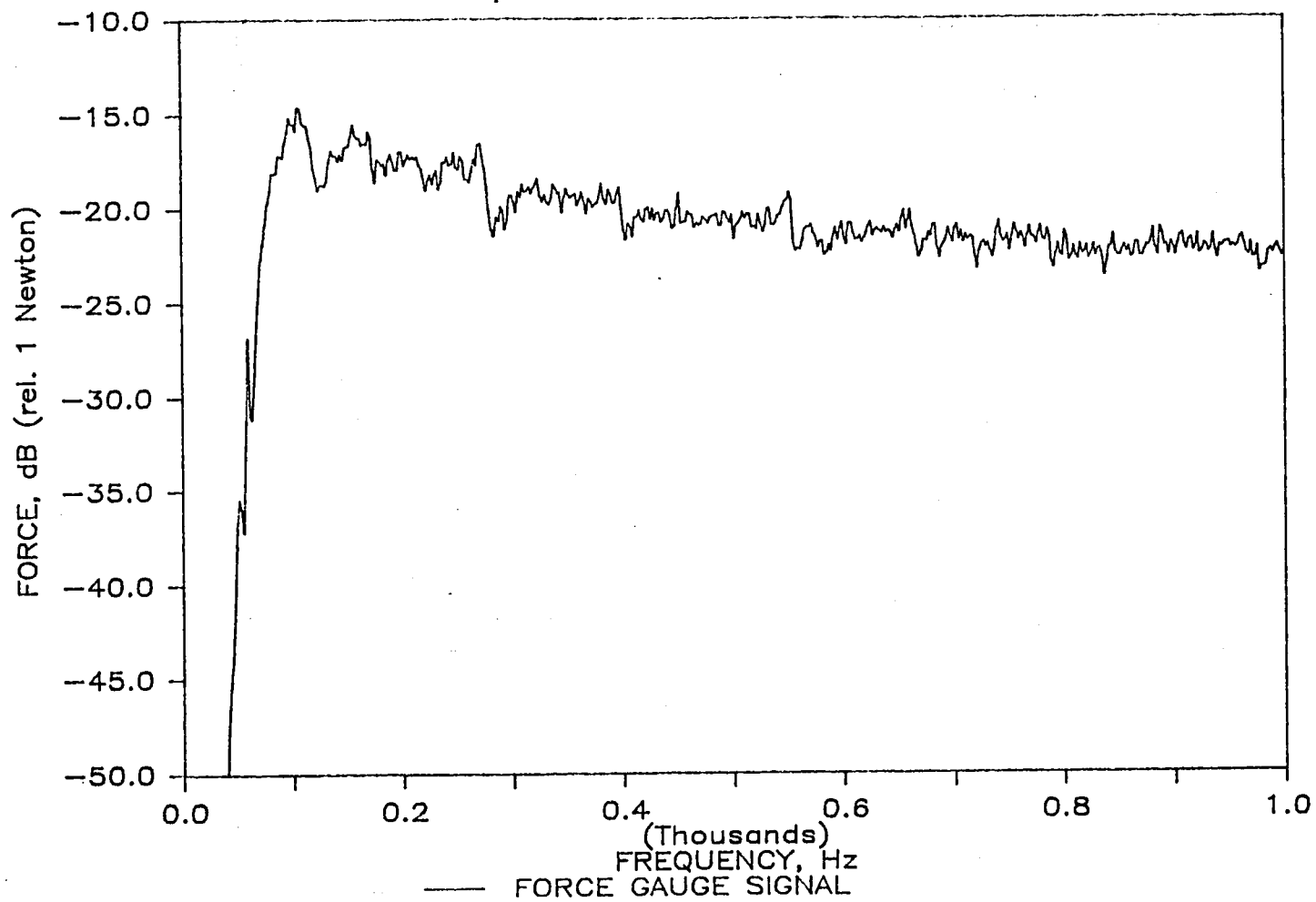


Figure 4 -- Forcing function produced by the shaker-rod-panel system.

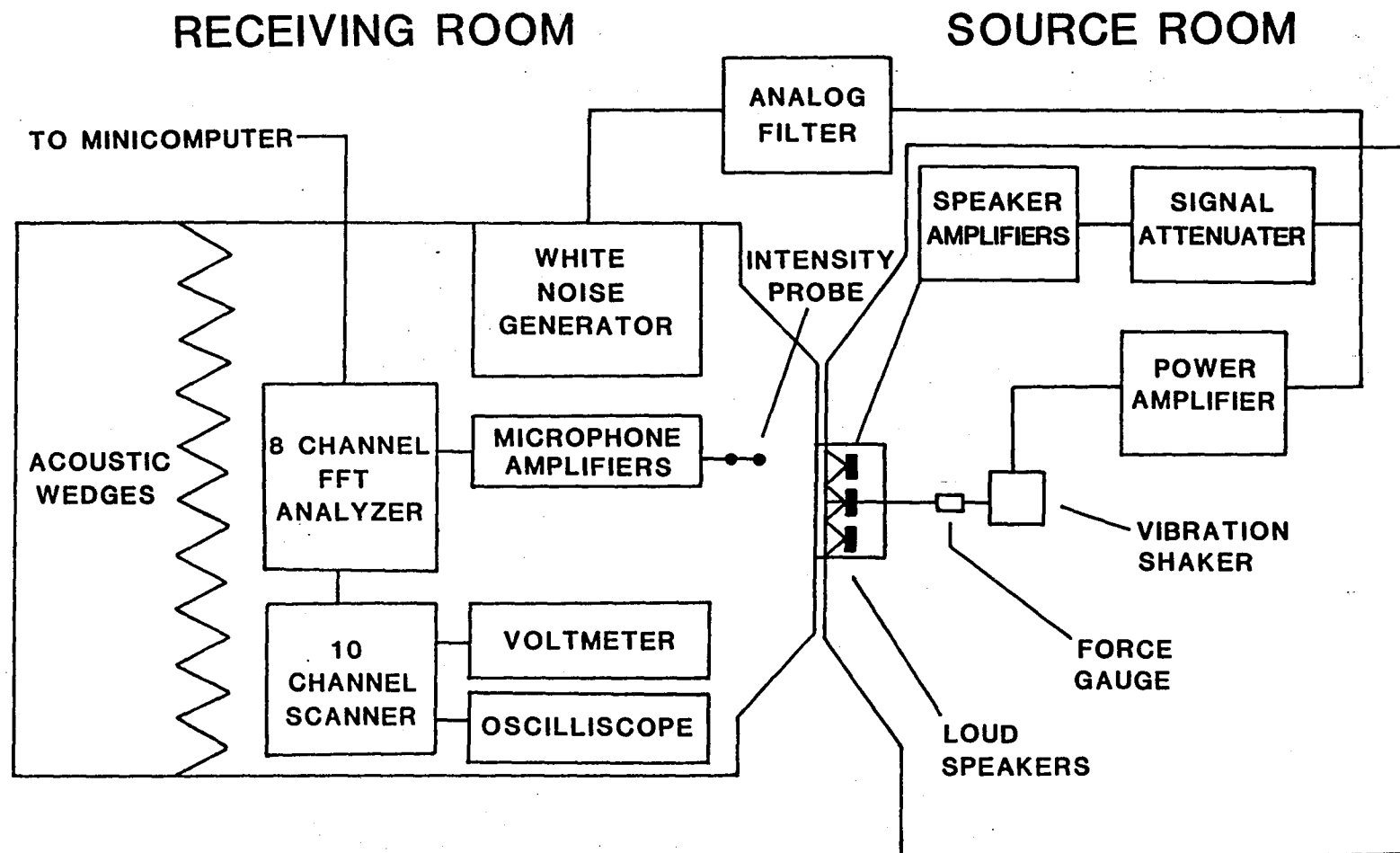


Figure 5 -- Block diagram of the instrumentation used for the measurements.

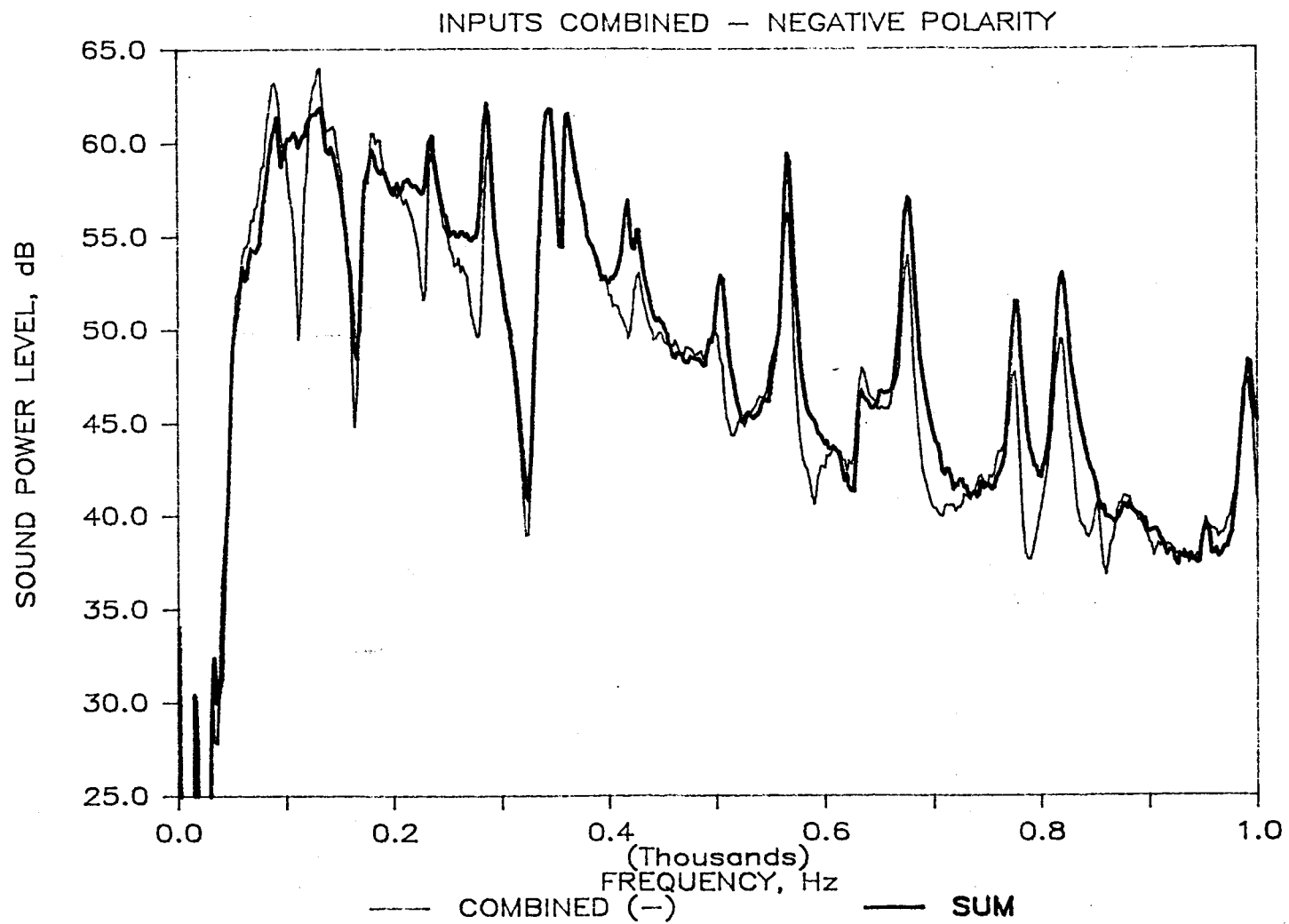


Figure 8 - Measured sound powers for combined inputs with the shaker located near the corner and negative polarity on the shaker.

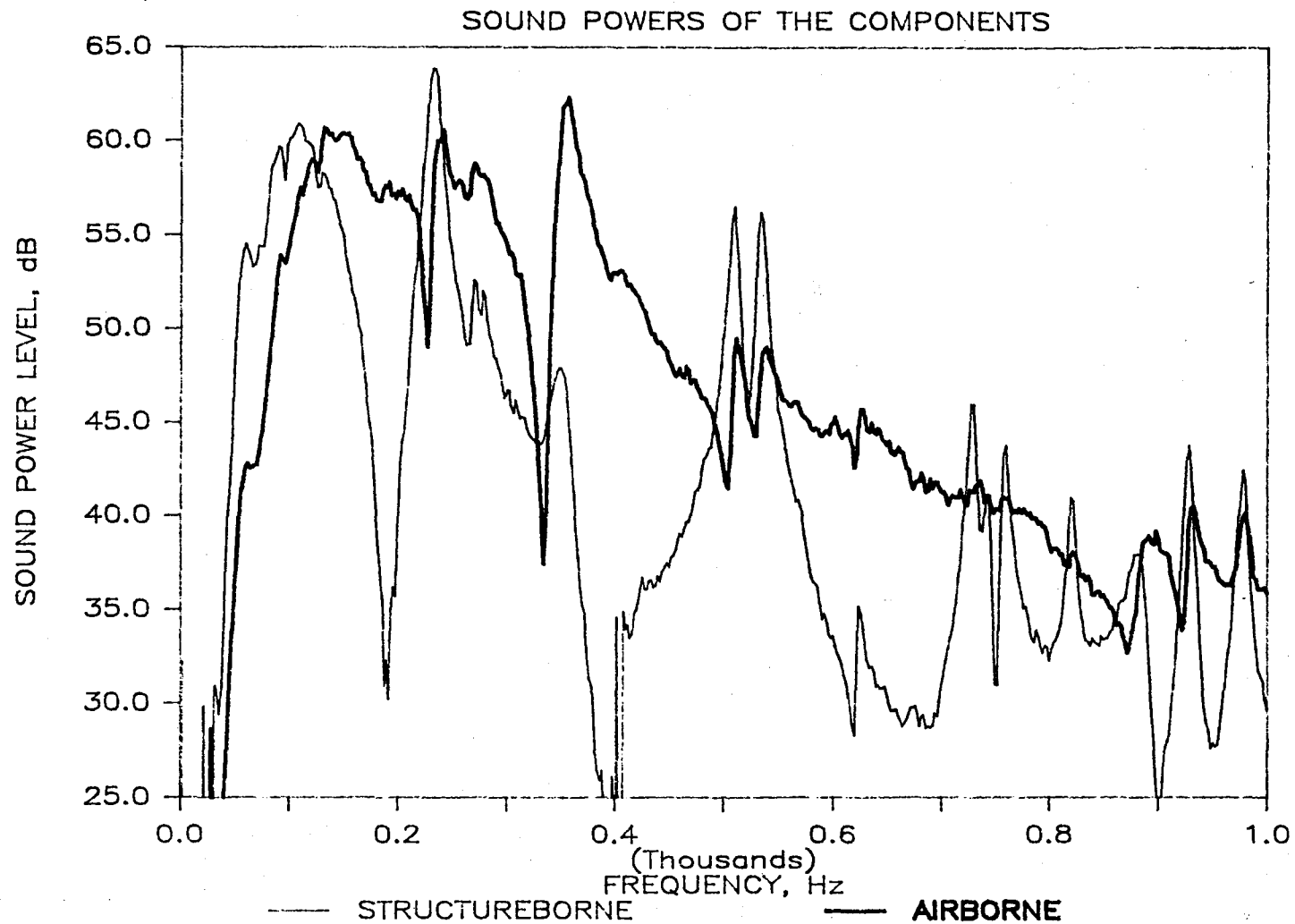


Figure 9 - Measured sound powers of the individual components with the shaker located at the center.

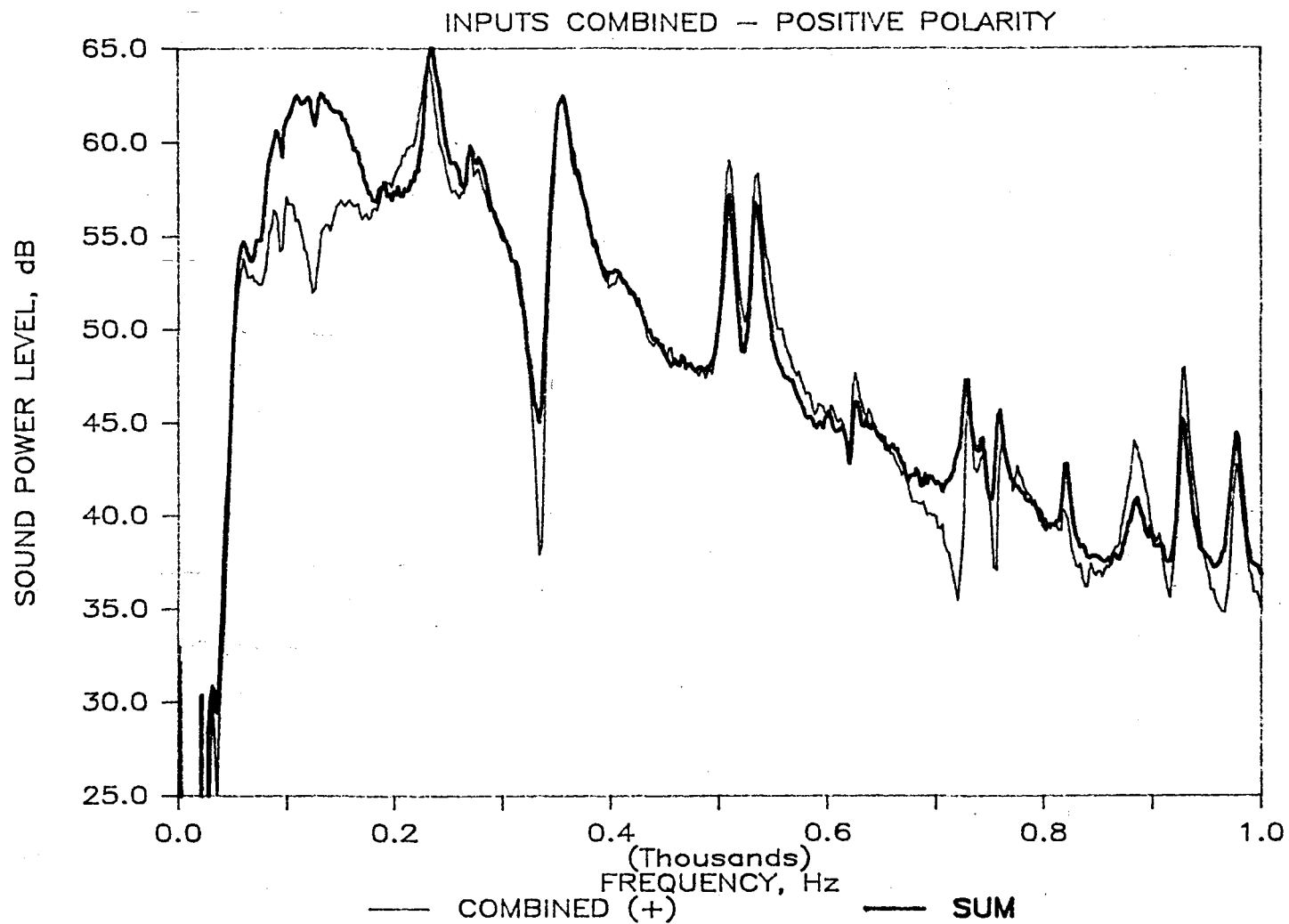


Figure 10 - Measured sound powers for combined inputs with the shaker located at the center and positive polarity on the shaker.

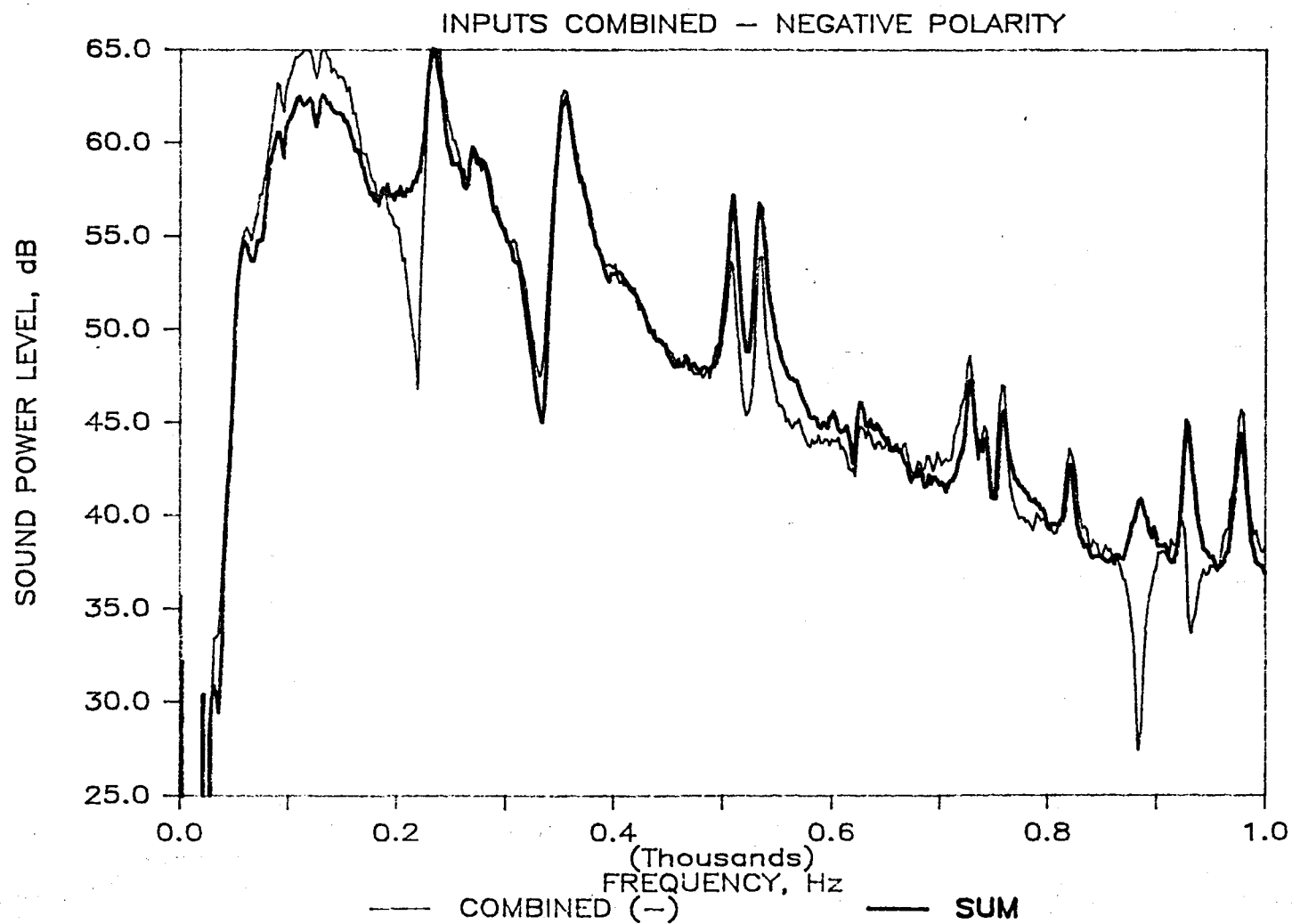


Figure 11 - Measured sound powers for combined inputs with the shaker located at the center and negative polarity on the shaker.

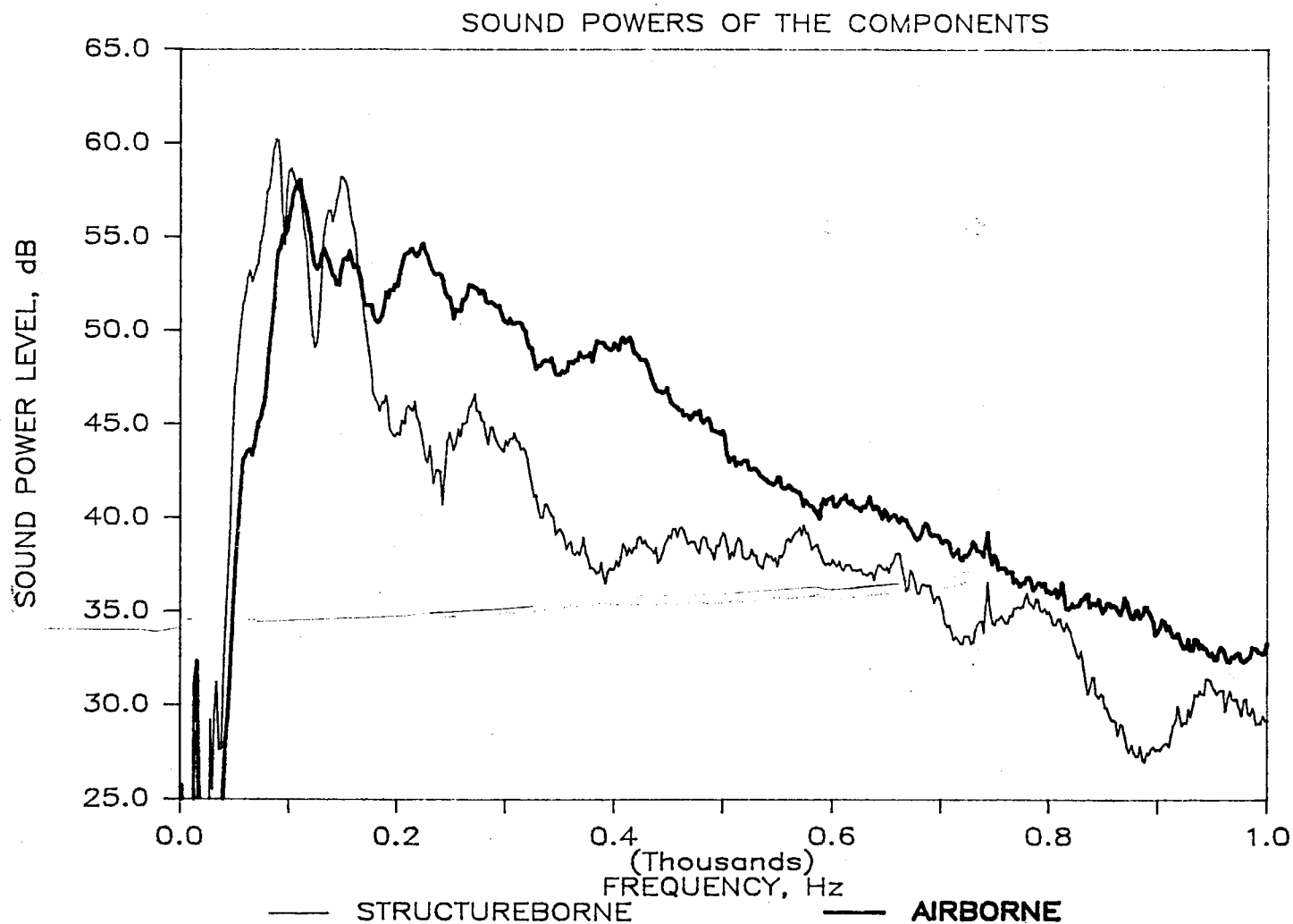


Figure 12 - Measured sound powers of the individual components with the shaker located near the corner and a moderate level of damping added to the panel.

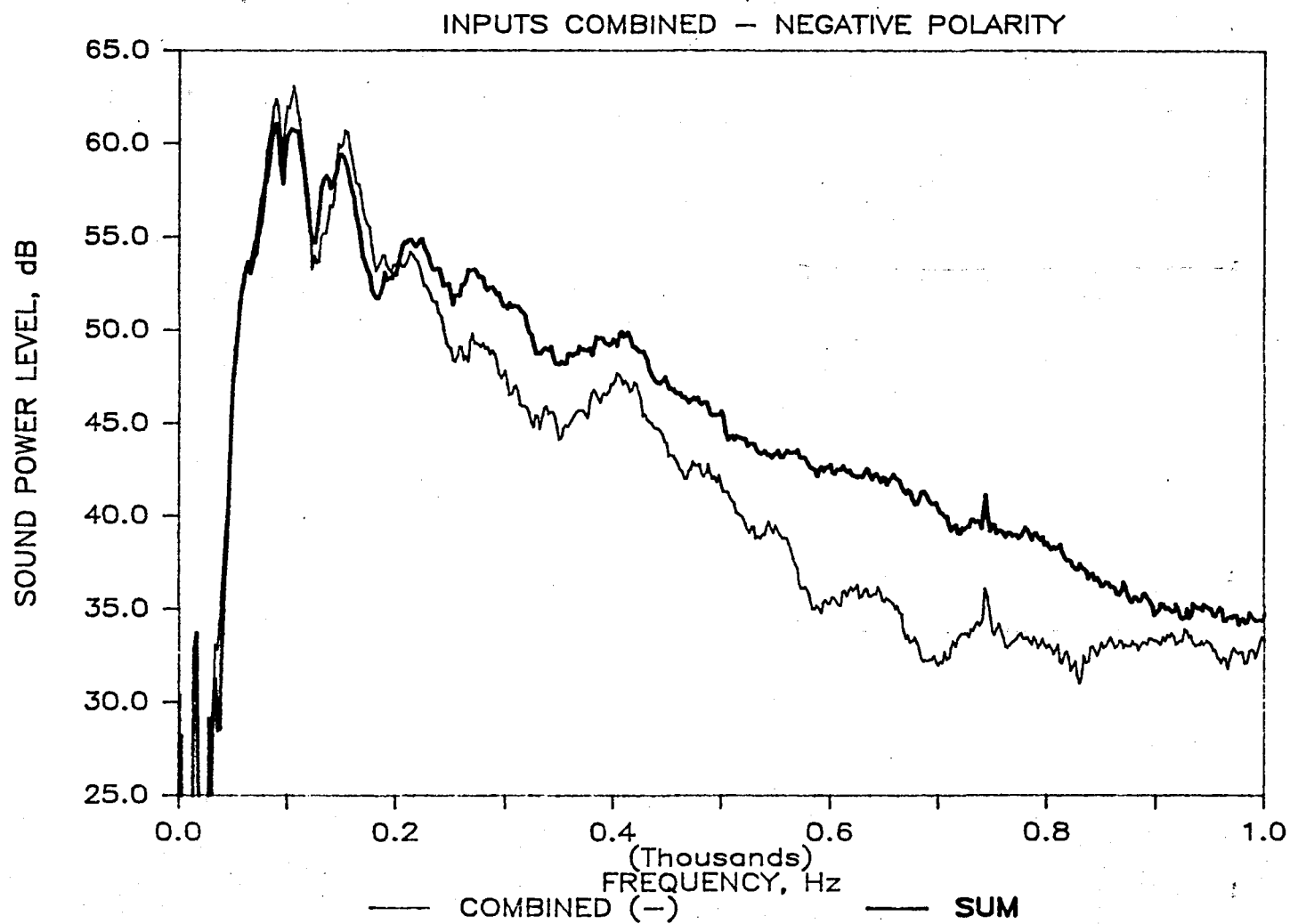


Figure 14 - Measured sound powers for combined inputs with the shaker located near the corner, moderate damping added to the panel, and negative polarity on the shaker.

1. Report No. NASA TM 87747		2. Government Accession No.		3. Recipient's Catalog No.	
4. Title and Subtitle Interaction of Airborne and Structureborne Noise Radiated by Plates, Volume II -- Experimental Study				5. Report Date July 1986	
				6. Performing Organization Code 505-63-11-02	
7. Author(s) Michael C. McGary				8. Performing Organization Report No.	
				10. Work Unit No.	
9. Performing Organization Name and Address NASA Langley Research Center Hampton, VA 23665-5225				11. Contract or Grant No.	
				13. Type of Report and Period Covered Technical Memorandum	
12. Sponsoring Agency Name and Address National Aeronautics and Space Administration Washington, DC 20546				14. Sponsoring Agency Code	
15. Supplementary Notes					
16. Abstract An experimental study was undertaken in order to further the understanding of the interaction of airborne and structureborne noise radiated by aircraft materials. The results of the study corroborate the findings of an earlier analytical study by showing that the noise radiation of vibrating plates due to combined airborne and structureborne inputs possesses a strong synergistic nature. The large influence of the interaction between the airborne and structureborne inputs has been hitherto ignored by researchers of aircraft interior noise problems.					
17. Key Words (Suggested by Author(s)) Aircraft Interior Noise Acoustic Intensity Airborne Noise Structureborne Noise			18. Distribution Statement Unclassified - Unlimited Subject Category - 71		
19. Security Classif. (of this report) Unclassified	20. Security Classif. (of this page) Unclassified	21. No. of Pages 35	22. Price A03		

End of Document